



Contents lists available at ScienceDirect

NeuroImage

journal homepage: www.elsevier.com/locate/ynimg

1 Encoding of event timing in the phase of neural oscillations

Q1 Anne Kösem^{a,b,c}, Alexandre Gramfort^{b,d,e}, Virginie van Wassenhove^{a,b,c,*}

3 ^a INSERM, U992, Cognitive Neuroimaging Unit, F-91191 Gif/Yvette, France

4 ^b CEA, DSV/I2BM, NeuroSpin Center, F-91191 Gif/Yvette, France

5 ^c Univ Paris-Sud, Cognitive Neuroimaging Unit, F-91191 Gif/Yvette, France

6 ^d INRIA, Parietal team, Saclay, F-91191 Gif-sur-Yvette, France

7 ^e LNAO, NeuroSpin, CEA Saclay, F-91191 Gif-sur-Yvette, France

8 A R T I C L E I N F O

9 Article history:

10 Accepted 4 February 2014

11 Available online xxxx

12 Keywords:

13 MEG

14 Oscillatory entrainment

15 Temporal order

16 Simultaneity

17 Internal clock

A B S T R A C T

Time perception is a critical component of conscious experience. To be in synchrony with the environment, the brain must deal not only with differences in the speed of light and sound but also with its computational and neural transmission delays. Here, we asked whether the brain could actively compensate for temporal delays by changing its processing time. Specifically, can changes in neural timing or in the phase of neural oscillation index perceived timing? For this, a lag-adaptation paradigm was used to manipulate participants' perceived audiovisual (AV) simultaneity of events while they were recorded with magnetoencephalography (MEG). Desynchronized AV stimuli were presented rhythmically to elicit a robust 1 Hz frequency-tagging of auditory and visual cortical responses. As participants' perception of AV simultaneity shifted, systematic changes in the phase of entrained neural oscillations were observed. This suggests that neural entrainment is not a passive response and that the entrained neural oscillation shifts in time. Crucially, our results indicate that shifts in neural timing in auditory cortices linearly map participants' perceived AV simultaneity. To our knowledge, these results provide the first mechanistic evidence for active neural compensation in the encoding of sensory event timing in support of the emergence of time awareness.

© 2014 Elsevier Inc. All rights reserved.

33 Introduction

34
35
36
37 While dedicated neural structures for time perception have been described (Buhusi and Meck, 2005; Coull et al., 2004; Harrington et al., 1998; Ivry and Schlerf, 2008; Morillon et al., 2009; Treisman et al., 1990; van Wassenhove, 2009; Wittmann, 2009, 2013), the encoding of sensory event timing has been proposed to result from the intrinsic dynamics of neural populations not necessarily dedicated to temporal processing (Johnston and Nishida, 2001; Karmarkar and Buonomano, 2007; van Wassenhove, 2009). For instance, the timing of a colored visual patch could be encoded in the dynamics of the neural population dedicated to the analysis of color (Karmarkar and Buonomano, 2007; Moutoussis and Zeki, 1997). In this non-dedicated view, the latency of neural responses could provide an index for event timing (Johnston and Nishida, 2001; Zeki and Bartels, 1998). Under this latency code hypothesis, timing mechanisms are based on the changes of neural routing delays in sensory areas coding for a specific sensory attribute (Moutoussis and Zeki, 1997; Zeki and Bartels, 1998). To date however, electroencephalographic (EEG) studies have reported little-to-no

54 correspondence between neural latencies and participants' perceived 55 timing (McDonald et al., 2005; Vibell et al., 2007), and rather suggest 56 that it is the phase of neural oscillations that plays a crucial role in the 57 encoding of visual event timing (Chakravarthi and Vanrullen, 2012; 58 Gho and Varela, 1988).

59 We here provide further evidence that the encoding of event timing 60 is realized in the phase of neural oscillations (in auditory cortex). It is 61 well known that distinct phases of low-frequency neural oscillations 62 are associated with periods of high and low neural excitability 63 (Buzsáki, 2010; Lakatos et al., 2008). These fluctuations have been 64 shown to impose temporal constraints on the "what" of perception by 65 modulating the perceptual detection threshold of various stimuli 66 (Busch et al., 2009; Fiebelkorn et al., 2013; Henry and Obleser, 2012; 67 Monto et al., 2008; Neuling et al., 2012). They have also been proposed 68 to serve parsing and informational chunking of sensory information 69 over time (VanRullen and Koch, 2003) notably for complex temporal 70 structures such as speech (Giraud and Poeppel, 2012). Indeed, neural 71 oscillations are known to be entrained to external rhythms (Rees 72 et al., 1986; Regan, 1966) and this entrainment may allow the align- 73 ment of cortical processing to the timing of sensory events (Giraud 74 and Poeppel, 2012; Schroeder and Lakatos, 2009). As such, this mecha- 75 nism naturally provides a means for the brain to internalize external 76 temporal regularities (Schroeder and Lakatos, 2009). In line with this 77 proposal, the phase of low-frequency neural oscillations has been

* Corresponding author at: CEADSVI2BM.NeuroSpin – INSERM Cognitive Neuroimaging Unit, NeuroSpin MEG, Brain Dynamics group, Bât 145 Point Courrier 156, F-91191 Gif sur Yvette, France.

E-mail address: Virginie.van.Wassenhove@gmail.com (V. van Wassenhove).

shown to reflect temporal expectancy or predictability of event timing (Stefanics et al., 2010). Here, we hypothesize that the brain could use oscillatory entrainment to establish a temporal reference frame and we thus ask whether the phase of entrained neural oscillations actually encodes the “when” of perception. Specifically, the preferred phase of oscillatory entrainment is known to be context-dependent (Besle et al., 2011; Gomez-Ramirez et al., 2011; Lakatos et al., 2008; Rees et al., 1986), suggesting that neural entrainment may not be a passive neural response. Additionally, preferential phases of entrained neural oscillations are subject-specific (Besle et al., 2011), making this neural index particularly well-suited for investigating the highly subjective and variable nature of time perception.

To test the specific hypothesis that the phase of an entrained neural oscillation directly informs on the variability of conscious timing, we transiently shifted participants' perceived timing using a lag-adaptation paradigm (Fujisaki et al., 2004; Miyazaki et al., 2006; Vroomen et al., 2004). Fig. 1 provides an overview of the experimental paradigm. During the induced changes of perceived timing, participants' brain activity was recorded with magnetoencephalography (MEG). During a given lag-adaptation block, audiovisual stimuli were presented rhythmically to induce an entrainment of oscillatory activity in sensory cortices. Analysis of MEG data showed that the preferential phase of entrained neural oscillations shifted during adaptation. Crucially, phase shifts of neural oscillatory entrainment in auditory cortex mirrored individuals' perceived simultaneity.

Materials and methods

Participants

Nineteen participants (7 females, mean age: 24 years old) took part in the study. All had normal or corrected-to-normal vision, normal color vision and normal hearing, and were naive as to the purpose of the study. Each participant provided a written informed consent in accordance with the Declaration of Helsinki (2008) and the Ethics Committee on Human Research at NeuroSpin (Gif-sur-Yvette, France). Three subjects were excluded from the study: one subject did not finish the experiment, and two were unable to perform the temporal order judgment task properly. A total of sixteen participants were thus considered for MEG analyses.

Stimuli

The experiment was written in Matlab using the Psychophysics toolbox (Brainard, 1997). Visual stimuli consisted of disks lasting 16.7 ms (1 frame). A visual annulus (9.5° of visual angle) consisted in the superposition of circles with different shades of gray. Visual stimuli were projected at a 60 Hz refresh rate onto a screen placed 90 cm away from participants seated under the MEG dewar. Auditory stimuli consisted of 16 ms duration white noise (incl. 5 ms fade-in and fade-out). Auditory stimuli were presented via Etymotic earphones (Etymotic Research Inc., USA).

Procedure

Two types of blocks were used in this experiment namely, lag-adaptation (3 conditions: S, A200V or V200A) and temporal order judgment (TOJ) blocks. In the lag-adaptation blocks (Fig. 1B), a series of simultaneous (S) or desynchronized audiovisual events were displayed (A200V: audition leading vision by 200 ms or V200A: vision leading audition by 200 ms). During the lag-adaptation block, a stream of 65 AV stimuli was presented. The stream of AV events was displayed at an average rate of 1 Hz; the stimulus onset asynchrony (SOA) between two successive auditory or visual stimuli was randomly chosen from a normal distribution with a mean of 1 s and a standard deviation of 100 ms: thus, each SOA has 95% probability to fall between 804 ms and 1196 ms. The first 20 AV events and the last 15 AV events in the stream were made up of stimuli with a constant temporal lag. Three lags were tested: in the S condition, AV stimuli were synchronously displayed (lag = 0 ms); in the A200V condition, the sound preceded the visual stimulus by 200 ms and in the V200A condition, the visual stimulus preceded the sound by 200 ms. During the lag-adaptation block, participants were asked to count the number of temporal deviants that were introduced in the middle part of the lag-adaptation block. Temporal AV deviants consisted of desynchronized AV stimuli that deviated from the constant lag introduced at the beginning of the block. This task was introduced to insure that participants attended the temporal dimension of the AV stream which was reported to enhance temporal recalibration effects (Heron et al., 2010). Crucially however, only the first 20 and last 15 AV stimuli are reported here namely the periods during which no temporal deviants were introduced. Each lag-adaptation block was systematically followed by a TOJ in which participants' subjective simultaneity of AV events was evaluated. In the TOJ blocks, AV stimuli were displayed with delays ranging from ± 317 , ± 217 , ± 133 , ± 67 , to 0 (a negative delay corresponds to the auditory leads and a positive delay corresponds to the visual leads). After each presentation of an AV pair, participants had to judge which of the sound or the visual event appeared first in a two alternative forced choice (2-AFC). Each condition was tested four times leading to a total of 36 trials in the TOJ blocks. The experiment started and ended with 4S blocks (i.e. 4 times S + TOJ). Other blocks were alternated between

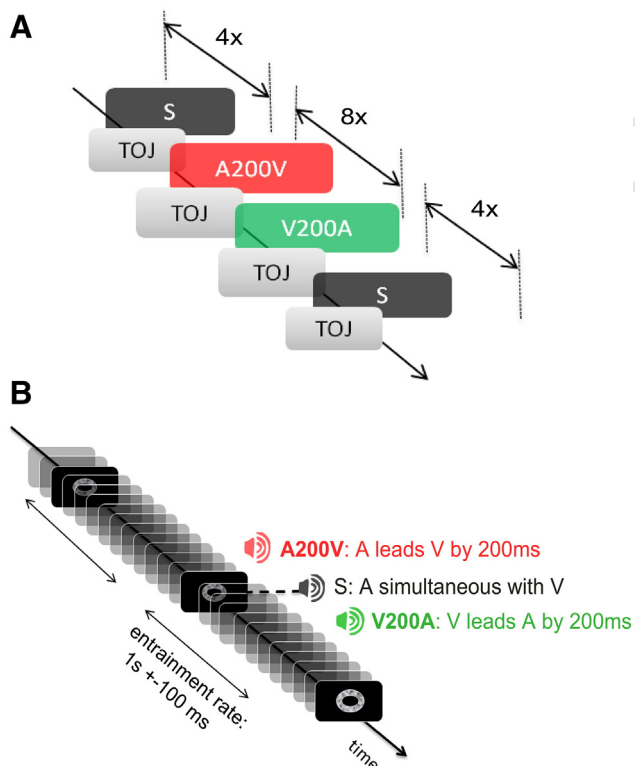


Fig. 1. Experimental design. (A) Three different audiovisual (AV) lag-adaptations were tested: simultaneous AV presentation (S, black), sound leading visual by 200 ms (A200V, red) and visual leading sound by 200 ms (V200A, green). Each lag-adaptation block was followed by a temporal order judgment (TOJ) block during which participants reported which of the auditory or visual event occurred first. One MEG session comprised eight blocks of each lag-adaptation (S, V200A and A200V). S blocks were run at the beginning and at the end of the MEG session; A200V and V200A alternated within the session. (B) In all lag-adaptation blocks, 65 AV stimuli were presented at an average rate of 1 Hz with a random jitter of ± 100 ms. This experimental manipulation was designed to elicit neural entrainment at 1 Hz in sensory cortices.

163 A200V and V200A condition. In total, each condition was run in 8 lag-
164 adaptation + TOJ blocks leading to a total of 24 blocks (Fig. 1A).

165 Data acquisition and preprocessing

166 MEG data acquisition

167 Brain magnetic fields were collected in a magnetically shielded
168 room using the whole-head Elekta Neuromag Vector View 306 MEG
169 system (Neuromag Elekta LTD, Helsinki) equipped with 102 triple-
170 sensor elements (two orthogonal planar gradiometers and one magne-
171 tometer per location). Participants were seated in the upright position.
172 Participants' head position was measured before each block with four
173 head position coils (HPI) placed over the frontal and mastoid areas.
174 Three fiducial points (nasion, left and right pre-auricular areas) and
175 were used during the digitization procedure to help coregistration
176 with anatomical MRI. MEG recordings were sampled at 1 kHz; band-
177 pass filtered between 0.03 Hz and 330 Hz and used Maxshield. The
178 electro-oculograms (EOG, horizontal and vertical eye movements)
179 and electrocardiogram (ECG) were simultaneously recorded with
180 MEG. Before each experiment, a so-called empty room recording of
181 about 1 min with no subject sitting under the dewar was acquired for
182 the computation of the noise covariance matrix.

183 MEG data preprocessing

184 The signal space separation (SSS) method was applied to decrease
185 the impact of external noise (Taulu et al., 2003). SSS correction, head
186 movement compensation, and bad channel rejection were done using
187 MaxFilter Software (Elekta Neuromag). Signal-space projection (SSP)
188 was computed by principal component analysis (PCA) using Graph soft-
189 ware (Elekta Neuromag) to correct for eye-blinks and cardiac artifacts
190 (Uusitalo and Ilmoniemi, 1997). A rejection criterion for epochs was ap-
191 plied for gradiometers with amplitude exceeding $4000 \text{ e}^{-13} \text{ T/m}$.

192 Structural MRI acquisition

193 Magnetic resonance imaging (MRI) was used to provide high-
194 resolution structural image of each individual's brain. The anatomical
195 MRI was recorded using a 3-T Siemens Trio MRI scanner. Parameters
196 of the sequence were: voxel size: $1.0 \times 1.0 \times 1.1 \text{ mm}$; acquisition
197 time: 466 s; repetition time $TR = 2300 \text{ ms}$; and echo time $TE = 2.98 \text{ ms}$.

198 Anatomical MRI segmentation

199 Volumetric segmentation of participants' anatomical MRI and corti-
200 cal surface reconstruction was performed with the FreeSurfer software
201 (<http://surfer.nmr.mgh.harvard.edu/>) (Dale et al., 1999; Fischl and
202 Dale, 2000). These procedures were used for group analysis with the
203 MNE suite software (<http://www.martinos.org/mne/>). Individuals' cur-
204 rent estimates were registered onto the FreeSurfer average brain for
205 surface based analysis and visualization.

206 Co-registration procedure (MEG-aMRI)

207 The co-registration of MEG data with the individual's structural MRI
208 was carried out by realigning the digitized fiducial points with MRI
209 slices. Using `mne_analyze` within the MNE suite, digitized fiducial points
210 were aligned manually with the multimodal markers on the automati-
211 cally extracted scalp of the participant. To insure reliable co-
212 registration, an iterative refinement procedure was then used to realign
213 all digitized points (about 30 more supplementary points distributed on
214 the scalp of the subject) with the individual's scalp.

215 Data analysis

216 MEG source reconstruction

217 Individual forward solutions for all source locations located on the
218 cortical sheet were computed using a 3-layers boundary element
219 model (BEM) (Hämäläinen and Sarvas, 1989) constrained by the indi-
220 vidual's anatomical MRI. Cortical surfaces extracted with FreeSurfer

were sub-sampled to about 5120 equally spaced vertices on each hemi-
221 sphere. The noise covariance matrix for each individual was estimated
222 from the raw empty room MEG recordings preceding the individual's
223 MEG acquisition. The forward solution, noise covariance and source co-
224 variance matrices were used to calculate the dSPM estimates (Dale et al.,
225 1999). The inverse computation was done using a loose orientation con-
226 straint (loose = 0.2, depth = 0.8) (Lin et al., 2006). The cortically
227 constrained reconstructed sources were then registered, morphed,
228 onto the FreeSurfer average brain for group-level statistical analysis
229 that was performed with MNE-python (Gramfort et al., 2013a, 2013b).
230

231 Labels of interest

232 We restricted the analysis to labels of interest in auditory and visual
233 sensory cortices in the right hemisphere on the average FreeSurfer brain
234 after morphing. Known hemispheric asymmetries in auditory cortex
235 have consequences on the signal-to-noise ratio of MEG recordings
236 across hemispheres (Shaw et al., 2013). Consistent with this, a great ma-
237 jority of our participants showed a higher and more reliable SNR in the
238 right hemisphere. Labels were drawn individually based on the follow-
239 ing two criteria: (i) maximal amplitude of the M100 response to audito-
240 ry (resp. visual) stimulus for the auditory (resp. visual) label; and
241 (ii) consistency with functional anatomy. Individuals' labels are pre-
242 sented in Fig. S2 superimposed on the FreeSurfer average brain.

243 Event-related fields and source reconstruction

244 Event-related fields (ERF) were computed by averaging 15 trials at
245 the beginning and at the end of a lag-adaptation block. Data were gath-
246 ered across the 8 lag-adaptation blocks for each asynchrony condition
247 (S, A200V, V200A). For auditory ERF, the stimulus onset was locked to
248 the sound onset; for visual ERF, the stimulus onset was locked to the vi-
249 sual stimulus. Data were segmented in epochs of 1 s (400 ms pre- and
250 600 ms post-stimulus onset). Baseline correction was applied using
251 the first 200 ms of the epoch (-400 to -200 ms pre-stimulus onset).
252 The inverse solver used to localize the sources was then applied on
253 the averaged normed evoked data. The normalization procedure was
254 done to alleviate source cancellation when averaging sources within a
255 label of interest, and across subjects (Gross et al., 2013). The compari-
256 sons of evoked responses between conditions were computed using a
257 non-parametric permutation test. Correction for multiple comparisons
258 was performed with cluster level statistics using as base statistic Stu-
259 dent *t*-test computed at each time sample (Maris and Oostenveld,
260 2007). Only temporal clusters with corrected *p*-value ≤ 0.05 are
261 reported.

262 Power spectrum analysis

263 Low-frequency components in the frequency spectra could either
264 originate from neural entrainment to the 1 Hz stimulation or from
265 noise having a power spectrum density with $1/f$ distribution. To sub-
266 stantiate a peak neural entrainment at 1 Hz, the $1/f$ component was re-
267 moved by subtracting at each frequency bin the mean power of the
268 neighboring frequency values 4 frequency values were: $[fo - 0.14\text{Hz};$ **Q4**
 $fo - 0.07 \text{ Hz}; fo + 0.07 \text{ Hz}; fo + 0.14 \text{ Hz}]$ (Nozaradan et al., 2011).
269

270 Phase analyses

271 The first 5 trials of each lag-adaptation block were discarded as they
272 established transient episodes before the establishment of the steady-
273 state regime (Capilla et al., 2011). Hence, an equal number of 15 trials
274 (or stimuli) at the beginning and at the end of a lag-adaptation period
275 were considered for analysis. Single trial data were convolved with a
276 3-cycle Morlet wavelet centered at 1 Hz with a full width at half maxi-
277 mum of the power in the frequency domain of $[0.7 \text{ Hz}, 1.3 \text{ Hz}]$ (Keil
278 et al., 2013) (Fig. 2). Epoch lengths were 4 s and centered on the visual
279 or on the auditory stimulus onset. From the coefficients obtained with
280 wavelet convolution the instantaneous phase at visual or auditory
281 onset was extracted (as indicated in the text where relevant). Subse-
282 quent analyses were done on the distribution of phase values across

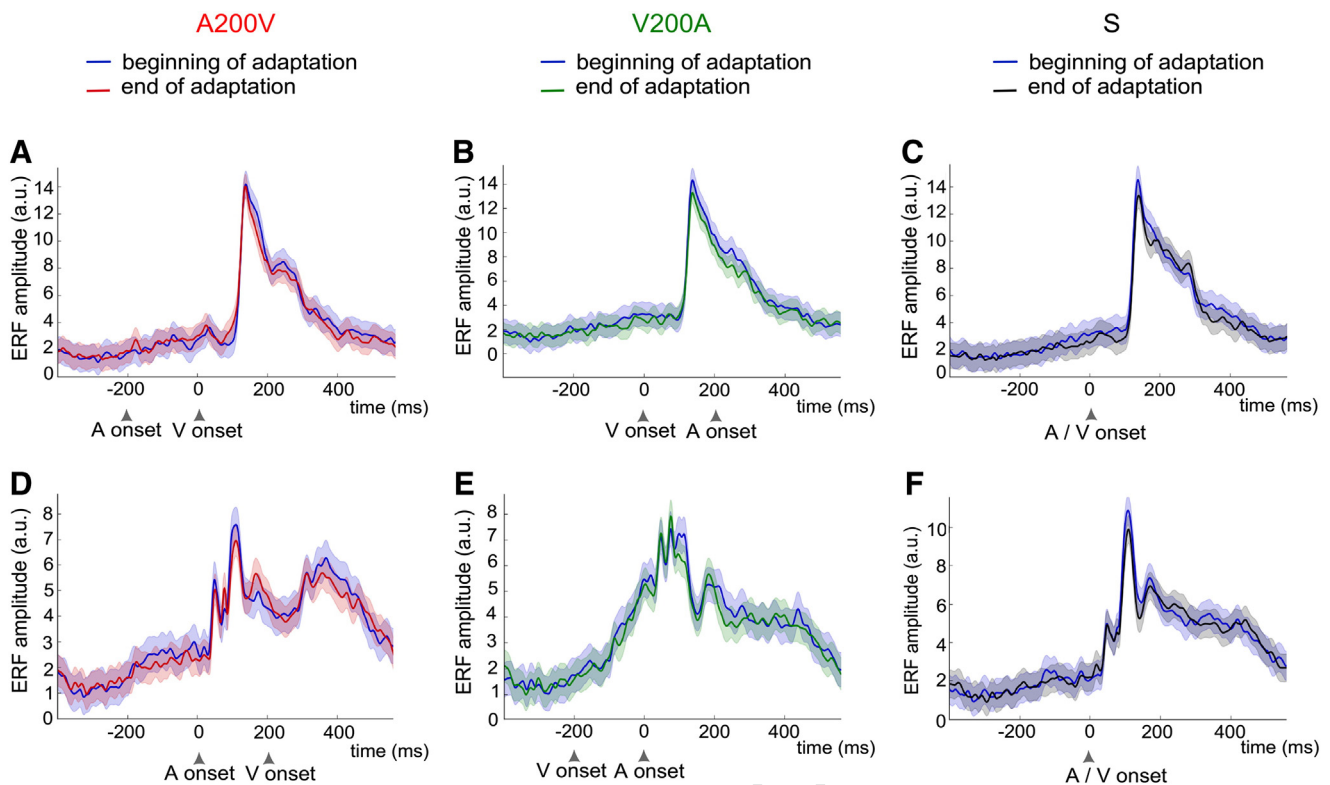


Fig. 2. Visual and auditory evoked responses before and after lag-adaptation. Auditory and visual evoked responses were obtained by separately time-averaging the first 15 trials at the beginning (blue) and at the end (A200V: red; V200A: green; S: black) of a given lag-adaptation block. Evoked responses were time-locked to the visual and auditory onsets in visual (A–C) and auditory cortices (D–F), respectively. Overall, no significant differences in the auditory or visual evoked response profiles were observed in the course of the lag-adaptation blocks, irrespective of the condition. Additionally, no significant influence of auditory stimuli was observed in the visual ERFs (A–C). In contrast, auditory evoked responses in A200V and V200A significantly differed ($p \leq 0.05$): in V200A, a ramping modulation of the auditory evoked responses was observed ~ 70 ms prior to sound onset whereas in A200V, a significant modulation of the auditory evoked responses at ~ 300 ms post-sound onset was observed.

283 trials gathered across specific condition, namely: the beginning or end
284 of a lag-adaptation period, conditions S, A200V or V200A and for each
285 participant.

286 Phase uniformity test

287 Phase distributions were submitted to Rayleigh's test for uniformity
288 of phase data (Fisher, 1995). A significant Rayleigh test ($p \leq 0.05$) indicates
289 that the distribution of phases shows a phase preference. If significance
290 was reached, the circular mean of each distribution was computed and used for
291 phase/ERFs and phase/behavior correlation analyses.

292 For each participant and each condition, a Rayleigh test was per-
293 formed. If all three conditions passed the test, entrainment was considered
294 to be true for that participant. When separating trials between the
295 beginning and the end of a lag-adaptation period, a criterion of two out
296 of three conditions passing the Rayleigh test was considered evidence
297 for entrainment.

298 The phase-locking value (PLV) (Lachaux et al., 1999) is defined as:

$$299 \text{ PLV}(t) = \frac{1}{K} \left| \sum_{k=1}^K e^{j\theta(t,k)} \right|$$

301 where K is the number of trials, and $\theta(t,k)$ is the instantaneous phase at
302 time t and trial k . PLVs were computed to assess intra-subject variability
303 in the preferential phase.

303 Statistical comparison of phase distributions

304 To assess statistical significance of phase shifts between 2 conditions
305 (e.g. A and B), bootstrap measure of 95% confidence interval was used
306 on the phase distribution of the paired differences A–B (Fisher, 1995).

Phase distributions A and B were statistically different if the mean of 307
the difference was statistically different from zero, i.e. if zero lies outside 308
the measured confidence interval ($p \leq 0.05$). 309

Psychophysics – point of subjective simultaneity 310

The percentage of “visual first” responses during the TOJ task follow- 311
ing the lag-adaptation period (S, V200A, and A200V) were plotted as a 312
function of AV asynchrony and fitted with a logistic regression to a sig- 313
moid function of the form: 314

$$\text{fit} = \frac{1}{1 + \exp\left(\frac{\text{data} - \text{PSS}}{\text{JND}}\right)}.$$

315 From each individual fit, the point of subjective simultaneity (PSS)
316 value and the just noticeable difference (JND) were estimated. The PSS 317
corresponds to the AV asynchrony at which an individual responds at 318
chance level (50%) in a TOJ task and thus taken as a true subjective si- 319
multaneity estimate (Vroomen and Keetels, 2010). 320

Results 321

Participants underwent a series of alternating lag-adaptation and 322
TOJ blocks while being recorded with MEG. Three AV delays were tested 323
(Figs. 1A–B): simultaneous AV presentations (S, control condition), a 324
sound leading a visual event by 200 ms (A200V) and a visual event lead- 325
ing a sound by 200 ms (V200A). Each TOJ block allowed establishing an 326
individual's psychometric curve following each lag-adaptation block as 327
well as deriving the progression of the individual's point of subjective si- 328
multaneity (PSS). Our hypothesis was that changes in neural activity 329
during lag-adaptation would predict changes in subjects' perceived 330

331 simultaneity. First, we tested the latency code hypothesis by comparing
332 the event-related responses at the beginning and at the end of the lag-
333 adaptation. We then tested the phase code hypothesis by comparing
334 the phase of the entrained neural oscillation at the beginning and the
335 end of the adaptation (Supplementary Fig. S1).

336 *Stable evoked activity in sensory cortices during adaptation*

337 Auditory and visual event-related fields (ERFs) were source-
338 reconstructed. The resulting time-source series were separately aver-
339 aged in the auditory and visual labels. In all three lag-adaptation con-
340 ditions, visual evoked responses were comparable with no significant
341 modulations of the visual evoked responses by auditory stimuli
342 (Figs. 2A–C). To the contrary, clear modulations of the auditory evoked
343 responses by the presence of visual stimuli were observed (Figs. 2D–F)
344 in both A200V and V200A. The auditory evoked response profiles in
345 A200V and V200A significantly differed ($p \leq 0.05$): in V200A, a ramping
346 modulation of the auditory evoked response was observed ~ 70 ms prior
347 to sound onset whereas in A200V, a significant modulation of the audi-
348 tory evoked response at ~ 300 ms post-sound onset was observed. The
349 modulations of the auditory evoked responses remained steady
350 throughout the lag-adaptation block and did not significantly differ be-
351 tween the beginning and the end of a given lag-adaptation block. If, as
352 hypothesized, changes in perceived timing were caused by changes in
353 the neural timing of auditory and visual cortices during lag-adaptation,
354 the latency of evoked activity did not appear to be a good candidate to
355 capture this change. These observations are in agreement with previous
356 findings on evoked-related-potential literature (McDonald et al., 2005).

357 *Non-stationarity of the entrained neural oscillations during lag-adaptation*

358 As predicted by the rate of AV stimulation during lag-adaptation,
359 neural activity over long time scales displayed periodic fluctuations at
360 1 Hz i.e. oscillatory entrainment or frequency-tagging: a characteristic
361 frequency peak at 1 Hz was clearly observable in auditory and visual
362 power spectra (Figs. 3B, D) and in single-trial data (Figs. 3A, C). No sig-
363 nificant changes in 1 Hz power were found between the beginning and
364 the end of a given lag-adaptation period irrespective of the experimen-
365 tal condition.

366 Additionally, 1 Hz oscillatory activity showed a significant phase-
367 locking in both sensory cortices. Phase preferences of the 1 Hz oscilla-
368 tion were tested using a Rayleigh test against uniformity ($p < 0.05$). At
369 the beginning of all lag-adaptation periods (S, A200V, and V200A),
370 phase preferences were found to be significant in both sensory cortices
371 for 15 participants; at the end of all lag-adaptation periods (S, A200V,
372 and V200A), significant phase preferences were found for all partici-
373 pants. For all conditions and in both sensory cortices, the observed
374 phase locking values (PLV, index of the variance of phase distributions)
375 did not significantly differ between the beginning and the end of each
376 lag-adaptation period (Supplementary Table S1). Altogether, these re-
377 sults show the existence of robust phase preferences in all conditions
378 throughout the course of the experiment.

379 However, and unlike the power of the entrained 1 Hz oscillation, the
380 phase of the 1 Hz oscillatory component did not appear to be stationary
381 over the course of the lag-adaptation period. Specifically, the neural re-
382 sponses evoked by the stimulus presentation arrived at different phases
383 of the 1 Hz oscillation (Figs. 4A, B). In the non-zero lag adaptations
384 (A200V and V200A), phases of the 1 Hz oscillation shifted in opposite
385 directions in visual and auditory cortices whereas in the control condi-
386 tion (S), no phase shifts were observed (Fig. 4C). Within a given block,
387 stimuli presented at the beginning of the adaptation were identical to
388 those presented at the end: as previously reported, and consistent
389 with the steady stimulation, no significant differences were observed
390 when contrasting the evoked responses at the beginning and at the
391 end of a given lag-adaptation period (Fig. 2). If neural entrainment
392 was a passive neural response, no changes in the preferential phase

would be predicted. Hence, the observed phase shifts in the entrained
oscillatory response suggest an active modulation of the entrained 1
Hz oscillation not easily accounted for by the unchanged event-related
responses.

Additional analyses were performed supporting the independence
of evoked activity and neural oscillatory phase shifts. If the evoked re-
sponses impacted the phase of neural oscillations at 1 Hz, a similar pat-
tern of phase shifts in neighboring frequency regions should be found by
virtue of evoked response being fixed-latencies and strongly phase-
locked signals. Weak-to-no phase locking and no significant phase shifts
were observed for 2 or 3 Hz neural oscillations (Supplementary Fig. S2).

404 *Encoding of subjective timing in the phase of neural oscillations*

405 Our main hypothesis states that shifts in the phase of neural oscilla-
406 tions during adaptation may reflect active changes in subjective timing.
407 To test this, we compared the shifts in the phase of neural oscillations
408 with perceptual reports (Figs. 5A, B). Consistent with previous reports
409 on TOJ paradigms (Love et al., 2013; Van Eijk et al., 2008), the average
410 PSS value in the zero-lag adaptation condition (S) was biased towards
411 sound-leading asynchronies: on average, participants required the audi-
412 tory event to lead the visual event by 38 ms to consider them as simul-
413 taneous (Fig. 5B). Following lag-adaptation to A200V and V200A,
414 participants required the sound to lead the visual event even more
415 with PSS values of -87 ms (significant main effect of lag-adaptation:
416 $F(2,30) = 10.1, p < 0.001$, significant contrast $PSS_{A200V} - PSS_S$; $p =$
417 0.002) and -69 ms ($PSS_{V200A} - PSS_S$; $p = 0.03$), respectively
418 (Fig. 5B). Thus, in both A200V and V200A, the sound needed to be
419 heard before the visual event to be perceived as simultaneous, but shifts
420 in perception were more pronounced in A200V than in V200A
421 ($PSS_{A200V} - PSS_S$, $p = 0.01$). From a neural processing point of view,
422 these results suggest that auditory analysis may be delayed during
423 lag-adaptation and/or visual analysis advanced in time. As seen in
424 Fig. 4C, the average phase shifts during A200V and V200A lag-
425 adaptations were consistent with these predictions: lag-adaptation
426 leads to a negative shift of the phase of auditory entrained oscillation
427 i.e. the 1 Hz response in auditory cortex shifted forward in time; con-
428 versely, the phase of the visual entrained oscillation positively shifted
429 suggesting that the 1 Hz entrained response shifted backward in time.

430 It is noteworthy that while the direction of the PSS shifts observed
431 after lag-adaptation to A200V was consistent with seminal reports on
432 temporal recalibration (Fujisaki et al., 2004; Vroomen et al., 2004), the
433 PSS following V200A lag-adaptation did not shift in the direction pre-
434 dicted by seminal temporal recalibration effects. Nevertheless, the latter
435 finding remains consistent with other lag-adaptation reports (Miyazaki
436 et al., 2006; Yamamoto et al., 2012) and major differences in experi-
437 mental design including the choice of task and the absence of re-
438 adapting trials in the TOJ assessment task could account for these
439 differences (Cai et al., 2012; Yamamoto et al., 2012). Specifically, remote
440 and recent stimulation histories are known to bias in opposite ways the
441 perception of incoming stimuli (Chopin and Mamassian, 2012) and con-
442 sistent with this, PSS shifts are distinctly influenced by the presence or
443 the absence of re-adapting trials (Cai et al., 2012). Here, we did not
444 include re-adapting trials during the TOJ blocks and stimuli were ran-
445 domly chosen between -316 ms and $+316$ ms, hence the primary in-
446 fluence on lag adaptation was the remote stimulation history i.e. the
447 lag-adaptation trials.

448 Here, we used lag-adaptation to generate shifts in an individual's
449 subjective timing. As expected, a large inter-individual variability was
450 observed in the individual's default PSS (control S, zero-lag adaptation)
451 and in the propensity of an individual to temporally adapt to
452 desynchronized AV stimuli (Figs. 5A, C). In order to test whether the
453 shifts in the phase of the 1 Hz neural oscillation were commensurate
454 with subjective simultaneity, we capitalized on this inter-individual
455 variability and compared individuals' PSS with the shifts in the
456 entrained neural oscillation in each sensory cortex. Strikingly, the

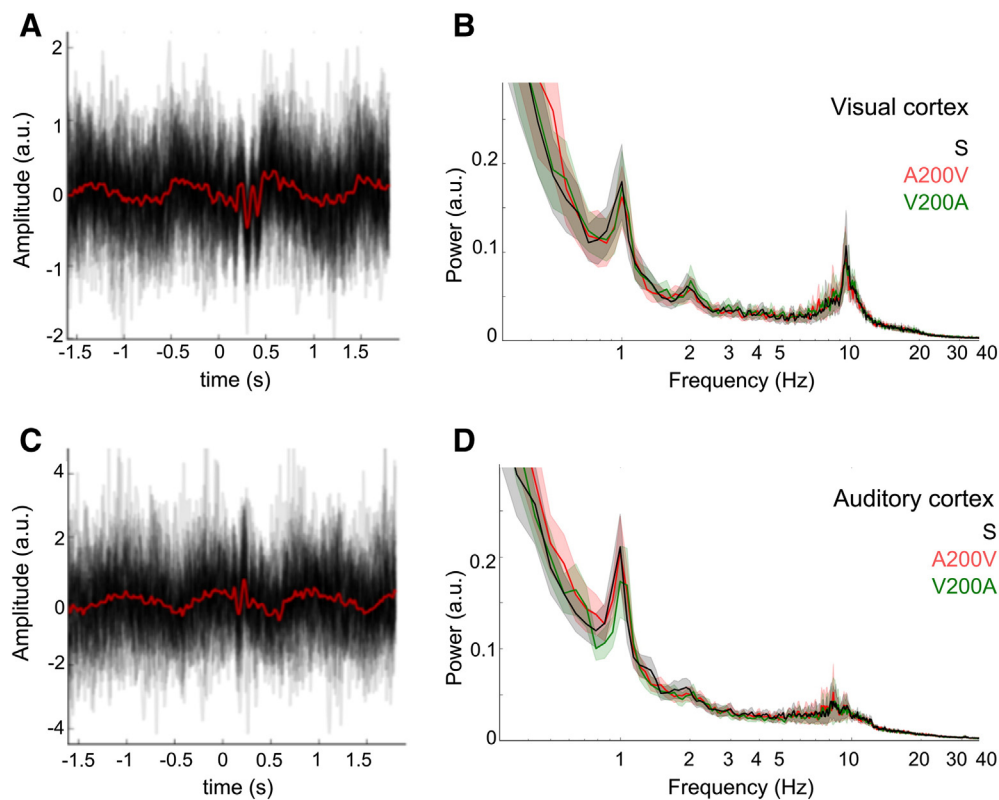


Fig. 3. Oscillatory entrainment and jitter procedure. In all lag-adaptation blocks, AV stimuli were presented at a rate of $1 \text{ Hz} \pm 100 \text{ ms}$. The temporal jitter was introduced to prevent full neural response time-locking and enable the dissociation of the oscillatory component from the evoked response (Lakatos et al., 2008). In both (A) and (C): one participant's superimposed single trial data (black) with the visual evoked response (red) at the end of A200V in visual cortex (A) and in auditory cortex (C). As can readily be seen in these two examples, the time-locked averaging of one stimulus (at zero) prevented to see the evoked responses of the preceding and following stimuli (which would be expected at about -1 and $+1$ s, respectively). As predicted, the temporal jittering procedure massively reduced the temporally adjacent evoked responses. Despite the absence of evoked response at -1 and $+1$ s, a clear single-trial oscillatory component at 1 Hz could be seen in both sensory cortices. In both (B) and (D): Frequency power spectra of neural responses in visual (B) and auditory (D) cortices for all lag-adaptation blocks. After $1/f$ correction (see Section 2.5.4.), a significant 1 Hz peak was readily observable (on sample t -test against $H_0 = \text{zero power}$, $p < 0.01$) in both sensory cortices. No significant differences in 1 Hz power were observed between the beginning and the end of the lag-adaptation periods irrespective of the experimental conditions. In visual cortices (panel B): S: $t(15) = -0.9$, n.s.; A200V: $t(15) = 0.6$, n.s.; and V200A: $t(15) = -0.7$, n.s. In auditory cortices (panel D): S: $t(15) = -1.8$, n.s.; A200V: $t(15) = 0.05$, n.s.; V200A: $t(15) = 1.7$, n.s.

457 phase shifts of the 1 Hz auditory oscillatory neural response significantly
 458 correlated with participants' subjective simultaneity whereas no such
 459 correlations were observed in visual cortices (Fig. 6). Specifically in au-
 460 ditory cortex, the more negative the phase of 1 Hz neural oscillation, the
 461 more the sounds needed to lead visual events to be perceived as simultane-
 462 ous. Thus a negative shift in phase, which corresponds to a forward
 463 neural timing i.e. a delay of 1 Hz auditory activity in time, is associated
 464 with a shift in perceived simultaneity towards auditory-lead asynchro-
 465 nies. Note that shifts in perception and shifts in neural timing
 466 change together in coherent directions: a delay in auditory processing
 467 as measured by a negative phase shifts should correspond to a perceived
 468 delay in auditory event timing; thus to perceive simultaneity the sound
 469 needs to be advanced in time i.e. the PSS is shifted towards auditory-
 470 lead asynchronies. Conversely, a positive phase shift moves the process-
 471 ing of auditory events backward in time thereby sounds have to lag visu-
 472 al events to be perceived as simultaneous. As reported in Fig. 6, the
 473 slope of the regression between perceived timing shift and neural
 474 timing shift was 1.2, suggesting that neural timing and perceived timing
 475 shifts are quantitatively similar. Additionally, the obtained regression
 476 predicts that a zero-phase shift in the 1 Hz neural oscillation observed
 477 in auditory cortex (i.e. stationarity or stable phase preference through
 478 time) should map onto a PSS of -45 ms . This value was very close to
 479 the mean PSS obtained experimentally in the control condition S
 480 (namely, -38 ms).

481 Overall these results suggest that AV simultaneity relies on asym-
 482 metrical cross-talks between auditory and visual sensory cortices,
 483 namely: auditory cortices actively adjust the timing of auditory events
 484 to match that of visual inputs.

Discussion

485

486 Shifts in perceived AV simultaneity following lag-adaptation
 487 (Fujisaki et al., 2004; Miyazaki et al., 2006; Vroomen et al., 2004;
 488 Yamamoto et al., 2012) have been hypothesized to originate from
 489 mechanisms capable of adjusting the neural processing time across sen-
 490 sory modalities (Fujisaki et al., 2004; Moutoussis and Zeki, 1997; Stone
 491 et al., 2001; Sugita and Suzuki, 2003; Zeki and Bartels, 1998). In support
 492 of this hypothesis, our study reveals that such mechanisms may be im-
 493 plemented as phase shifts of neural oscillations: contrasting the sensory
 494 responses before and after AV lag-adaptation provided no evidence for a
 495 latency code hypothesis and instead revealed significant phase shifts of
 496 the entrained 1 Hz neural oscillations. Crucially, it is the phase shifts of
 497 the auditory response that linearly predicted participants' shifts of sub-
 498 jective AV simultaneity and no systematic mapping was found between
 499 visual responses and subjective AV timing. The present findings thus
 500 suggest that auditory cortex temporally calibrates its window of analy-
 501 sis with respect to vision and that event timing linearly maps onto the
 502 phase of entrained neural oscillations.

Neural oscillations as pacemakers for the encoding of time

503

504 The "internal clock" is a prominent model of time perception which
 505 is classically composed of a pacemaker (ticking mechanism), an accu-
 506 mulator (of ticks) and a counter (Church, 1984; Treisman, 1963). Of par-
 507 ticular interest here, the pacemaker consists of an oscillator ticking at a
 508 frequency that can be modulated depending on the temporal properties
 509 of sensory stimuli (Buhsu and Meck, 2009; Treisman, 1984; Treisman
 510 509

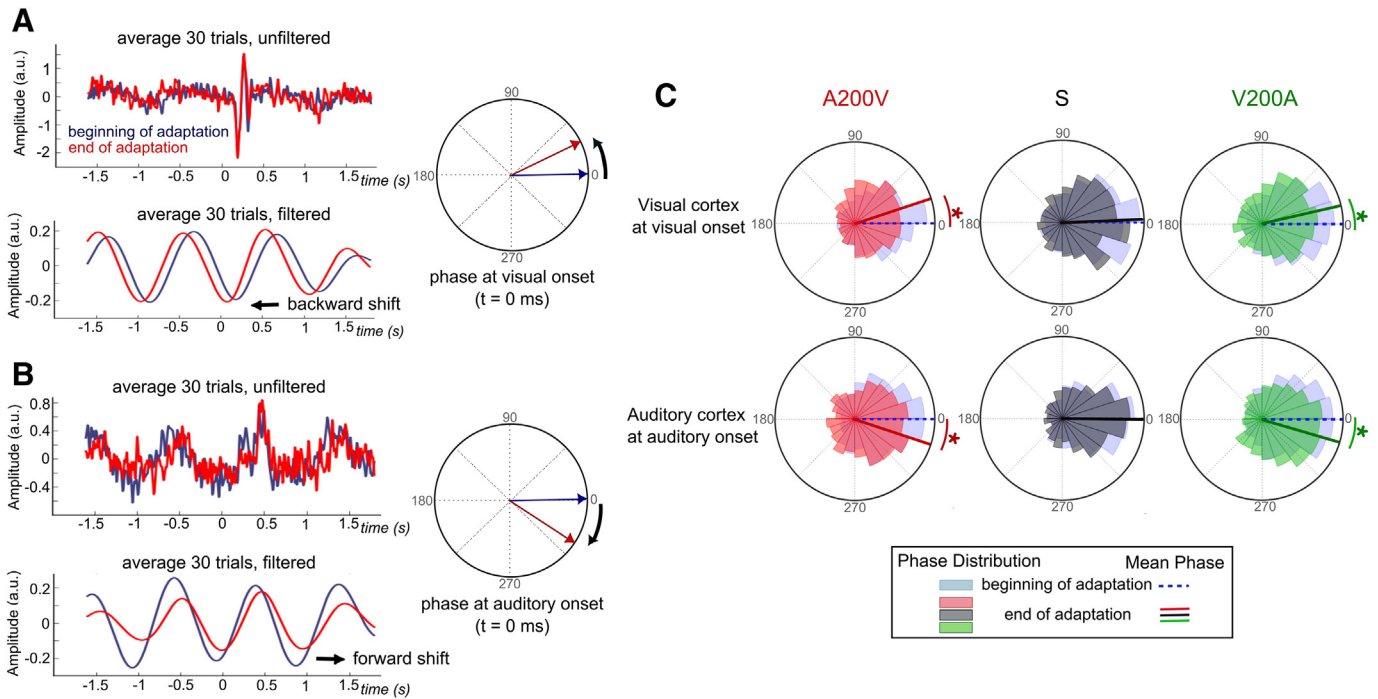


Fig. 4. 1 Hz neural response: oscillatory phase differences during lag-adaptation. (A) One participant's visual evoked response obtained at the beginning (blue) and at the end (red) of an A200V lag-adaptation block. The top graph shows the unfiltered visual evoked response; the bottom graph shows the same visual evoked response band-pass filtered from 0.5 to 1.5 Hz. The 1 Hz oscillatory component at the end of the lag-adaptation block (red) shows a backward shift in time with respect to the same oscillatory component at the beginning of the lag-adaptation (blue); this backward temporal shift is quantified as an increase in the mean instantaneous phase value across the 30 single trials used to compute the evoked response (right panel). (B) One participant's auditory evoked response at the beginning (blue) and at the end (red) of an A200V lag-adaptation block. The unfiltered and 0.5–1.5 Hz band-pass filtered auditory evoked responses are depicted in the top and bottom graph, respectively. The 1 Hz oscillatory component at the end of the lag-adaptation block (red) shows a forward shift in time with respect to the same oscillatory component at the beginning of the lag-adaptation (blue). The mean instantaneous phase across the 30 trials used to build the auditory evoked response shows a decrease between the beginning and the end of the block (right panel). (C) Instantaneous phase distribution and preferential instantaneous phase of the entrained 1 Hz neural oscillatory response at the beginning (light gray) and at the end (colored) of a given lag-adaptation block (S: black; A200V: red; V200A: green). Phase distributions were computed at visual onset in visual cortices (top) and at sound onset in auditory cortices (bottom). Phase distributions were individually normalized to the preferred instantaneous phase observed at the beginning of a given lag-adaptation block. Hence, all phase distributions at the beginning of a given block are centered on zero. In S, the phase distributions remained stable over time in both auditory ($+1^\circ$, 95% confidence interval (CI) = $[-6^\circ, +5^\circ]$) and visual (-1° , CI = $[-6^\circ, +8^\circ]$) cortices. In the desynchronized blocks, the mean instantaneous phase shifted in opposite directions in the auditory and visual cortices during lag-adaptation: specifically, in A200V the preferential phase in visual cortices increased ($+19^\circ$ or -53 ms, CI = $[12^\circ, 26^\circ]$) suggesting a backward shift in time of the entrained 1 Hz oscillatory response, whereas a forward shift in time was observed in auditory cortices (-19° or $+53$ ms, CI = $[-27^\circ, -9^\circ]$). Conversely, in V200A the mean instantaneous phase in visual cortices increased ($+16^\circ$ or -44 ms, CI = $[7^\circ, 25^\circ]$) but decreased in auditory cortices (-19° or $+53$ ms, CI = $[-26^\circ, -13^\circ]$). Hence, and as predicted, lag-adaptation to simultaneous AV stimuli (S) did not affect the phase of the entrained 1 Hz neural oscillation in sensory cortices whereas desynchronized AV stimuli (A200V and V200A) shifted the preferential phase distribution in opposite direction in the auditory and visual cortices.

et al., 1990, 1992): specifically, external temporal regularities can impose modulations of the pacemaker frequency so as to entrain the internal clock (Treisman et al., 1992). Similarly, intrinsic neural oscillations match the temporal scales of perceptual phenomena (Buzsáki and Draguhn, 2004; Roopun et al., 2008; van Wassenhove, 2009; Wang, 2010) and can be entrained to external rhythms (Rees et al., 1986; Regan, 1966). As such, neural oscillations have been hypothesized as natural pacemakers for conscious time estimation (Buhusi and Meck, 2005; Pöppel, 1997; Treisman et al., 1990; Varela et al., 1981). However, within this framework, a major problem for the brain is to determine when events occur with respect to its internal frame of reference. Our results suggest that the timing of events could automatically be encoded in the phase of a recruited pacemaker or entrained oscillation (thereby acting as a temporal frame of reference for cortex) and that the variation of the pacemaker's phase over time results in variation of perceived timing.

526 A canonical role for the phase of intrinsic and entrained neural oscillations?

527 It is noteworthy that we specifically targeted the delta range using
528 neural entrainment or frequency-tagging. EEG studies have previously
529 tested the idea that the order of visual events was coded in the phase
530 of the alpha oscillatory component (Gho and Varela, 1988) and recent
531 studies have pointed out to the role of theta/alpha in temporal visual
532 illusions (Chakravarthi and Vanrullen, 2012; VanRullen et al., 2006).

533 These studies suggest that intrinsic oscillations are recruited for the
534 encoding of events in the absence of external temporal regularities. Re-
535 cent hypotheses further extend the notion that the phase of low-
536 frequency neural oscillations is crucial for the encoding of order – for
537 instance with the implication of the theta band in working memory
538 (Lisman and Jensen, 2013) – or even for temporal parsing – for instance,
539 in speech (Giraud and Poeppel, 2012). The temporal encoding mecha-
540 nisms described in our experiment are de facto constrained by the
541 rhythmicity of the external inputs; in turn, however, the encoding of
542 event timing may capitalize on the temporal features provided by exter-
543 nal stimulation to build a temporal reference frame or pacemaker con-
544 sistent with the rhythms provided by the external sensory world.
545 While delta oscillations have been previously linked to temporal pre-
546 dictability (Stefanics et al., 2010), further investigations need to be
547 done to test their implication in the encoding of event timing when no
548 rhythmic stimulation or external temporal reference frame is provided.

549 Evoked activity and attention to time

550 Latency-based descriptions of cognitive functions classically use
551 event-related potentials/fields (ERP and ERF, respectively) to describe
552 the timing at which mental operations take place in cortex (Coles and
553 Rugg, 1995; Madl et al., 2011). The auditory and visual evoked re-
554 sponses were thus expected to partly reflect participants' perceptual
555 shifts in AV simultaneity taking place during lag-adaptation. However,

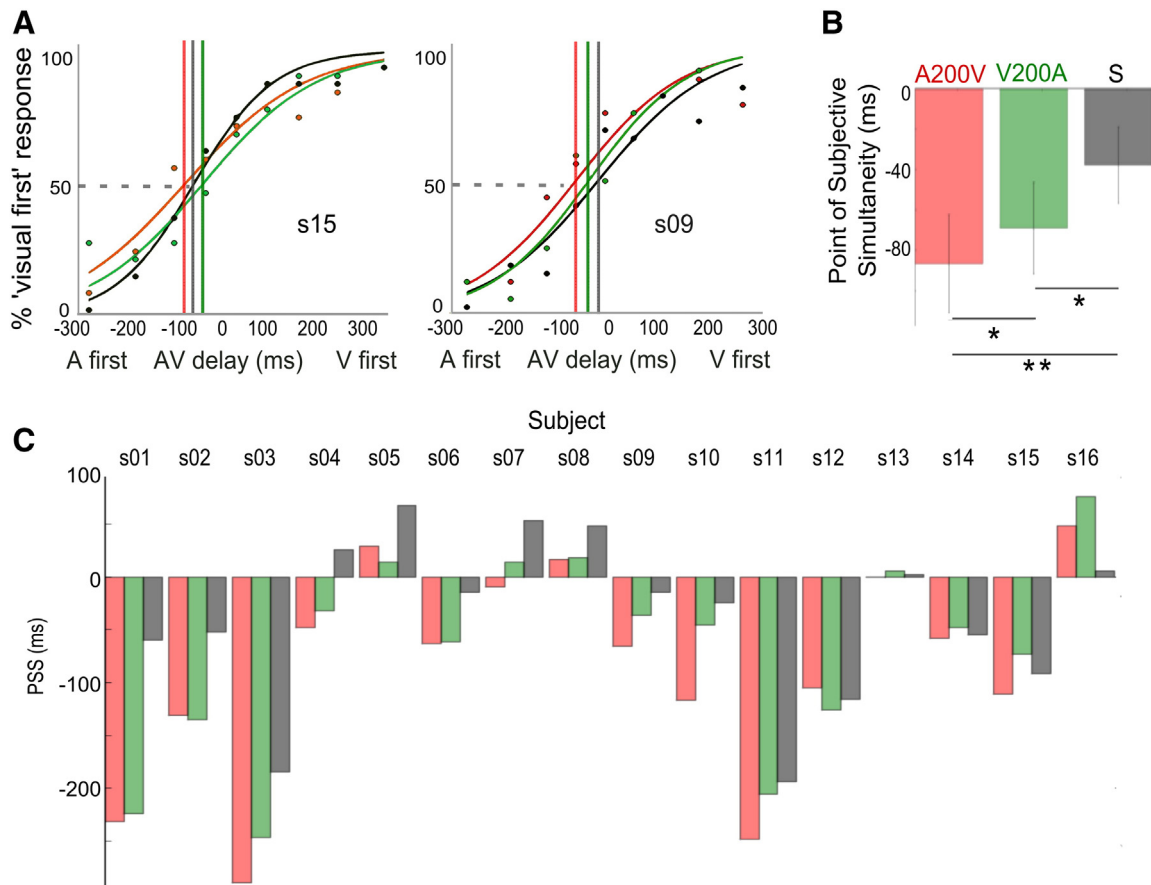


Fig. 5. Psychophysical results. (A) Two individuals' psychometric curves fitted to the percentage of "visual first" responses as a function of AV delays in the TOJ blocks. The negative and positive AV delays are audio leads (visual lags) and audio lags (visual leads), respectively. The individual's points of subjective simultaneity (PSS) observed after each lag-adaptation block are indicated by a colored line: TOJ obtained in S, A200V and V200A are in black, red and green, respectively. (B) Grand average PSS ($n = 16$). The control condition S showed a mean TOJ value of -38 ± 19 ms, suggesting that on average a sound had to be presented about 38 ms before a visual event to be perceived as synchronous. Following lag-adaptations to A200V and V200A, significant shifts of PSS towards audio leads were observed compared to the control condition (A200V: -87 ± 24 ms; V200A: -69 ± 23 ms). Errors bars reflect s.e.m. (C) Summary of all individuals' PSS. As can readily be observed, a large inter-individual variability was obtained in the individuals' PSS values (control blocks (S)) and in the propensity of a given individual to temporally shift his or her natural PSS.

and surprisingly, no significant changes in the amplitude or in the latency of the evoked responses were observed in the course of lag-adaptation, albeit clear visual modulations of the auditory responses were seen. Previous EEG studies using auditory and tactile stimuli during a TOJ task reported amplitude modulation (McDonald et al., 2005) or latency shifts (Vibell et al., 2007) of the evoked sensory responses as a function of which sensory modality was attended. It was notably reported that attention could speed up the processing of the attended sensory modality. Here, no systematic changes in the evoked profiles were observed suggesting that during lag-adaptation participants equally paid attention to the auditory and visual events as per task requirements (cf. methods).

Although the lack of significant lag-adaptation suppression (Grill-Spector et al., 2006) of the evoked responses was surprising, it is classically known that attention can attenuate the effect of neural suppression (Gazzaley et al., 2005). Here, participants were asked to pay attention to any deviants presented in the auditory, visual or audiovisual modalities during lag-adaptation. The lack of repetition suppression in both sensory cortices may thus be an index of successful attentional orienting. Additionally, recent findings have shown that the more temporally predictable, the higher the repetition suppression effects notably in the auditory responses (Costa-Faidella et al., 2011; Summerfield et al., 2008, 2011). In the context of predictive coding models, it has also been suggested that repetition and expectation were dissociable (Todorovic and de Lange, 2012). The current experimental design did not allow us to dissociate the factor of predictability and expectation

but these observations provide an alternative speculation, namely that paying attention to time may alleviate neural lag-adaptation.

One relevant point here is the integrative vs. segregative nature of the task with regard to multisensory processing: experimental paradigms using multisensory integration have classically reported an increase of sensory evoked responses, for instance when using the sound-induced flash illusion (Mishra et al., 2007; Watkins et al., 2006). In a TOJ task however, the segregation of auditory and visual information is a pre-requisite for successful ordering of auditory and visual events in time. Participants were repeatedly presented with AV lags at an entrainment rate consistent with automatic multisensory integration (Kösem and van Wassenhove, 2012): as such, audiovisual binding was reinforced in this task and an increased evoked response would have been expected. However, and at the same time, a decrease of the evoked responses was expected by virtue of neural suppression (Grill-Spector et al., 2006). Hence, one possible explanation for the absence of significant modulations of the sensory evoked responses in the course of adaptation is the competition between the integrative and segregative processes in this particular experimental design. Additional work will be required to further address this working hypothesis.

Phase of neural oscillations: encoding time (or space?)

Multisensory integration is known to capitalize on the spatiotemporal coincidence of sensory events (Colonius and Diederich, 2010; Meredith et al., 1987) and visual capture of auditory spatial representation is a

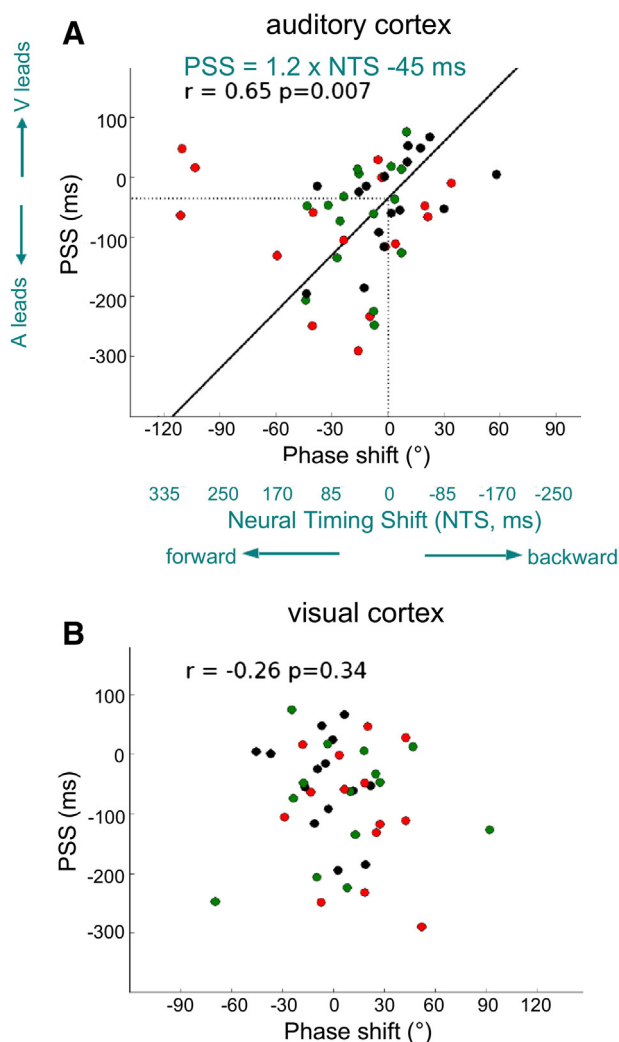


Fig. 6. Phase shifts reflect subjective timing. Individuals' PSS were plotted as a function of the difference in mean instantaneous phase (end minus beginning in a given lag-adaptation period) in auditory (A) and visual cortices (B). Each data point corresponds to an individual duplet, namely: the mean phase difference obtained in a given lag-adaptation period (S: black; A200V: red; V200A: green) and the associated individual's PSS measured during the following TOJ block. A linear regression was computed on a per individual basis between the mean PSS and the circular mean of the instantaneous phases of the 1 Hz neural oscillation obtained across lag-adaptation blocks. A significant correlation was found between the phase shifts of the entrained 1 Hz neural oscillation in auditory cortices and individuals' PSS ($r = 0.65$, $p < 0.01$) whereas no such correlation was found in visual cortices ($r = -0.26$, n.s.).

classic phenomenon (i.e. ventriloquism, (Alais and Burr, 2004; Lewald and Guskı, 2003; Slutsky and Recanzone, 2001)) well accounted for by Bayesian models of multisensory integration (Alais and Burr, 2004; Burr and Alais, 2006; Ernst and Bühlhoff, 2004; Witten and Knudsen, 2005). More generally, vision tends to be most reliable in encoding spatial cues whereas audition provides the most reliable temporal cues. In the experimental design used here, visual events were displayed at a constant distance on the monitor screen whereas sounds were presented via headphones. By virtue of spatiotemporal coincidence and given the consistent AV timing over lag-adaptation, the auditory distance would have to be adjusted to visual information. In a scheme analogous to the calibration of auditory spatial representation by vision in the barn owl (Knudsen and Brainard, 1991), the observed non-stationary phase shifts in auditory cortices could thus reflect an automatic means to fine tune spatiotemporal coincidence across sensory modalities. Specifically, auditory spatial uncertainty could be compensated for by the stable spatiotemporal reference frame established in vision. From this viewpoint, the auditory

system would not act as a timer per se; rather, the distance of auditory events would be actively made compatible with visual inputs to form an integrated AV percept. Hence, shifts in AV simultaneity may reflect the compensation of temporal delays in audition. Such mechanism would predict what we observed, namely that the entrainment of auditory and visual cortices is asymmetrical when attention is directed to the timing of events (i.e. to the dominant sensory modality for timing, namely audition); it also predicts that response times for audition (but not for vision) vary during AV delay exposure (Navarra et al., 2009) as well as the correlation between reaction times and visual to auditory phase-reset previously described (Thorne et al., 2011). Our results further support a recent discussion on the functional asymmetry between the sampling of acoustic and visual information over time (Thorne et al., 2011), namely: while the visual system may naturally rely on endogenous rhythms (e.g. alpha oscillations, Gho and Varela, 1988; Jensen et al., 2012; VanRullen and Koch, 2003; Varela et al., 1981) and overt sampling (e.g. (micro)saccades, Schroeder and Lakatos, 2009), the auditory system may necessitate temporal-locking to incoming acoustic inputs to accurately represent information over time (Giraud and Poeppel, 2012; Henry and Obleser, 2012; Stefanics et al., 2010; Thorne et al., 2011). Hence, while visual timing may rely on an internally generated temporal reference frame, audition may require the establishment of a temporal reference frame on the go and locked to the temporal statistics of the auditory environment.

Neural oscillations: multiplex encoding of information

Our results suggest that, in cortex, the phase of neural oscillations may provide an automatic means to flag events in a brain's referential time — i.e. provide the needed brain-centric view of time (Scharnowski et al., 2013). The encoding of spatiotemporal information in the phase of neural oscillations has been described in the hippocampus in which mechanisms of phase precession encode spatial locations as the animal navigates in a maze (Buzsáki, 2002; Lisman, 2005; Skaggs et al., 1995). Phase precession mechanisms may not be exclusive to hippocampal networks nor to spatial processing and may serve a more general purpose such as encoding events for working memory while preserving temporal order (Lisman, 2005; Lisman and Jensen, 2013). In particular, the content of a sensory event is encoded by the neural assembly firing within a certain gamma cycle (Lisman, 2005; Lisman and Jensen, 2013) while the relative timing of the event is encoded in the phase of the theta oscillation (Lisman, 2005; Lisman and Jensen, 2013).

In cortex, low-frequency neural oscillations are known to regulate the excitability of neural ensembles such that specific phases of low-frequency neural oscillations are associated with periods of high and low neuronal excitability (Buzsáki, 2010; Lakatos et al., 2008; Schroeder and Lakatos, 2009): the phase of low-frequency neural oscillations modulates the power of high-frequency neural oscillatory responses, a mechanism known as phase-power or cross-frequency coupling (Canolty et al., 2006). Neural synchronizations in higher frequency ranges (e.g. gamma range, $>40 \text{ Hz}$) provide a reliable index of feature binding within and across sensory modalities (Arnal et al., 2011; Engel et al., 1991; Roelfsema et al., 1997; Senkowski et al., 2008; Tallon-Baudry and Bertrand, 1999). In multisensory integration, low-frequency neural oscillations (delta, 1–2 Hz) play a crucial role in the temporal selection (Besle et al., 2011; Fiebelkorn et al., 2013; Gomez-Ramirez et al., 2011; Lakatos et al., 2008; Schroeder and Lakatos, 2009) and in the integration of AV information (Fiebelkorn et al., 2011; Kösem and van Wassenhove, 2012; Luo et al., 2010).

Hence, the phase of low-frequency oscillations may provide the fine-grained temporal resolution needed for the segregation of AV event timing and conscious timing while preserving integration processes through neural synchronization (necessary in building the mental representation of a multisensory AV object).

In such scheme, the informational chunking operates over an oscillatory cycle by eliciting temporal windows of high neural excitability for

integration (Panzeri et al., 2010; van Wassenhove, 2009), while the phase of neural oscillations provides the temporal stamping operation needed to preserve the timing of operations in parallel systems. As such, the same informational content can be encoded in a multiplexed manner with (i) integration operating on those sensory attributes used in the building of an internal object (Engel and Singer, 2001; Treisman, 1996) while (ii) segregation – or temporal stamping – provides the automatic encoding of event timing. Such temporal encoding framework comes in support of intrinsic and non-dedicated models of time perception over small time scales (Karmarkar and Buonomano, 2007). Our data further converge with recent findings showing that accurate phase encoding of the temporal structure of sensory events affords predictability (Schroeder and Lakatos, 2009; Stefanics et al., 2010) and support recent phase-coding approaches in computational neurosciences (Nadasdy, 2010).

Conclusion

We showed that perceived simultaneity linearly maps onto the phase of neural oscillations in the auditory cortex. Our findings complement recent findings showing that accurate phase encoding of temporal event structure affords predictability (Schroeder and Lakatos, 2009; Stefanics et al., 2010) and enhances task performance (Busch et al., 2009; Monto et al., 2008; Neuling et al., 2012; Romei et al., 2012; Varela et al., 1981). Our results further suggest that mechanisms analogous to phase precession in the hippocampus may be used in cortex for the encoding of event timing. Specifically, the phase of slow oscillatory activity in sensory areas may provide a canonical means to organize sensory inputs in time. Future work will address the possibility that a canonical function of neural oscillations is the encoding of event timing serving the emergence of psychological time.

Supplementary data to this article can be found online at <http://dx.doi.org/10.1016/j.neuroimage.2014.02.010>.

Acknowledgments

This work was supported by an ERC-YStG-263584, an ANR10JCJC-1904 and an IRG-249222 to V.vW. We are grateful to the NeuroSpin infrastructure groups, for their support in participant recruitment; and to anonymous reviewers for their comments on prior version of the manuscript.

Conflict of interest

The authors report no conflict of interest.

References

Alais, D., Burr, D., 2004. The ventriloquist effect results from near-optimal bimodal integration. *Curr. Biol.* 14, 257–262.

Arnal, L.H., Wyart, V., Giraud, A.-L., 2011. Transitions in neural oscillations reflect prediction errors generated in audiovisual speech. *Nat. Neurosci.* 14, 797–801.

Besle, J., Schevon, C.A., Mehta, A.D., Lakatos, P., Goodman, R.R., McKhann, G.M., Emerson, R.G., Schroeder, C.E., 2011. Tuning of the human neocortex to the temporal dynamics of attended events. *J. Neurosci.* 31, 3176–3185.

Brainard, D.H., 1997. The Psychophysics toolbox. *Spat. Vis.* 10, 433–436.

Buhusi, C.V., Meck, W.H., 2005. What makes us tick? Functional and neural mechanisms of interval timing. *Nat. Rev. Neurosci.* 6, 755–765.

Buhusi, C.V., Meck, W.H., 2009. Relativity theory and time perception: single or multiple clocks? *PLoS One* 4, e6268.

Burr, D., Alais, D., 2006. Combining visual and auditory information. *Prog. Brain Res.* 155, 243–258.

Busch, N.A., Dubois, J., VanRullen, R., 2009. The phase of ongoing EEG oscillations predicts visual perception. *J. Neurosci.* 29, 7869–7876.

Buzsáki, G., 2002. Theta oscillations in the hippocampus. *Neuron* 33, 325–340.

Buzsáki, G., 2010. Neural syntax: cell assemblies, synapsembles, and readers. *Neuron* 68, 362–385.

Buzsáki, G., Draguhn, A., 2004. Neuronal oscillations in cortical networks. *Science* 304, 1926–1929.

Cai, M., Stetson, C., Eagleman, D.M., 2012. A neural model for temporal order judgments and their active recalibration: a common mechanism for space and time? *Front. Psychol.* 3, 470.

Canolty, R.T., Edwards, E., Dalal, S.S., Soltani, M., Nagarajan, S.S., Berger, M.S., Barbaro, N.M., Knight, R.T., 2006. High gamma power is phase-locked to theta oscillations in human neocortex. *Science* 313, 1626–1628.

Capilla, A., Pazo-Alvarez, P., Darriba, A., Campo, P., Gross, J., 2011. Steady-state visual evoked potentials can be explained by temporal superposition of transient event-related responses. *PLoS One* 6.

Chakravarthy, R., Vanrullen, R., 2012. Conscious updating is a rhythmic process. *Proc. Natl. Acad. Sci. U. S. A.* 109, 10599–10604.

Chopin, A., Mamassian, P., 2012. Predictive properties of visual adaptation. *Curr. Biol.* 22, 622–626.

Church, R.M., 1984. Properties of the internal clock. *Ann. N. Y. Acad. Sci.* 423, 566–582.

Coles, M., Rugg, M., 1995. Event-Related Brain Potentials: An Introduction. In: Coles, M., Rugg, M. (Eds.), *Electrophysiology of Mind: Event-Related Brain Potentials and Cognition*. Oxford University Press, London, pp. 1–26.

Colonius, H., Diederich, A., 2010. The optimal time window of visual-auditory integration: a reaction time analysis. *Front. Integr. Neurosci.* 4, 11.

Costa-Faidella, J., Baldeweg, T., Grimm, S., Escera, C., 2011. Interactions between “what” and “when” in the auditory system: temporal predictability enhances repetition suppression. *J. Neurosci.* 31, 18590–18597.

Coull, J.T., Vidal, F., Nazarian, B., Macar, F., 2004. Functional anatomy of the attentional modulation of time estimation. *Science* 303, 1506–1508.

Dale, A.M., Fischl, B., Sereno, M.I., 1999. Cortical surface-based analysis. I. Segmentation and surface reconstruction. *NeuroImage* 9, 179–194.

Engel, A.K., Singer, W., 2001. Temporal binding and the neural correlates of sensory awareness. *Trends Cogn. Sci.* 5, 16–25.

Engel, A.K., König, P., Singer, W., 1991. Direct physiological evidence for scene segmentation by temporal coding. *Proc. Natl. Acad. Sci. U. S. A.* 88, 9136–9140.

Ernst, M.O., Bühlhoff, H.H., 2004. Merging the senses into a robust percept. *Trends Cogn. Sci.* 8, 162–169.

Fiebelkorn, I.C., Foxe, J.J., Butler, J.S., Mercier, M.R., Snyder, A.C., Molholm, S., 2011. Ready, set, reset: stimulus-locked periodicity in behavioral performance demonstrates the consequences of cross-sensory phase reset. *J. Neurosci.* 31, 9971–9981.

Fiebelkorn, I.C., Snyder, A.C., Mercier, M.R., Butler, J.S., Molholm, S., Foxe, J.J., 2013. Cortical cross-frequency coupling predicts perceptual outcomes. *NeuroImage* 69, 126–137.

Fischl, B., Dale, A.M., 2000. Measuring the thickness of the human cerebral cortex from magnetic resonance images. *Proc. Natl. Acad. Sci. U. S. A.* 97, 11050–11055.

Fisher, N.I., 1995. *Statistical Analysis of Circular Data*. Cambridge University Press, Cambridge.

Fujisaki, W., Shimojo, S., Kashino, M., Nishida, S., 2004. Recalibration of audiovisual simultaneity. *Nat. Neurosci.* 7, 773–778.

Gazzaley, A., Cooney, J.W., Rissman, J., D’Esposito, M., 2005. Top-down suppression deficit underlies working memory impairment in normal aging. *Nat. Neurosci.* 8, 1298–1300.

Gho, M., Varela, F.J., 1988. A quantitative assessment of the dependency of the visual temporal frame upon the cortical rhythm. *J. Physiol. Paris* 83, 95–101.

Giraud, A.-L., Poeppel, D., 2012. Cortical oscillations and speech processing: emerging computational principles and operations. *Nat. Neurosci.* 15, 511–517.

Gomez-Ramirez, M., Kelly, S.P., Molholm, S., Sehatpour, P., Schwartz, T.H., Foxe, J.J., 2011. Oscillatory sensory selection mechanisms during intersensory attention to rhythmic auditory and visual inputs: a human electrocorticographic investigation. *J. Neurosci.* 31, 18556–18567.

Gramfort, A., Luessi, M., Larson, E., Engemann, D.A., Strohmeier, D., Brodbeck, C., Goj, R., Jas, M., Brooks, T., Parkkonen, L., Hämäläinen, M., 2013a. MEG and EEG data analysis with MNE-python. *Front. Neuroinformatics* 7.

Gramfort, A., Luessi, M., Larson, E., Engemann, D.A., Strohmeier, D., Brodbeck, C., Parkkonen, L., Hämäläinen, M.S., 2013b. MNE software for processing MEG and EEG data. *NeuroImage*.

Grill-Spector, K., Henson, R., Martin, A., 2006. Repetition and the brain: neural models of stimulus-specific effects. *Trends Cogn. Sci.* 10, 14–23.

Gross, J., Baillet, S., Barnes, G.R., Henson, R.N., Hillebrand, A., Jensen, O., Jerbi, K., Litvak, V., Maess, B., Oostenveld, R., Parkkonen, L., Taylor, J.R., van Wassenhove, V., Wibral, M., Schoffelen, J.-M., 2013. Good practice for conducting and reporting MEG research. *NeuroImage*.

Hämäläinen, M.S., Sarvas, J., 1989. Realistic conductivity geometry model of the human head for interpretation of neuromagnetic data. *IEEE Trans. Biomed. Eng.* 36, 165–171.

Harrington, D.L., Haaland, K.Y., Knight, R.T., 1998. Cortical networks underlying mechanisms of time perception. *J. Neurosci.* 18, 1085–1095.

Henry, M.J., Obleser, J., 2012. Frequency modulation entrains slow neural oscillations and optimizes human listening behavior. *Proc. Natl. Acad. Sci. U. S. A.* 109, 20095–20100.

Heron, J., Roach, N.W., Whitaker, D., Hanson, J.V.M., 2010. Attention regulates the plasticity of multisensory timing. *Eur. J. Neurosci.* 31, 1755–1762.

Ivry, R.B., Schlerf, J.E., 2008. Dedicated and intrinsic models of time perception. *Trends Cogn. Sci.* 12, 273–280.

Jensen, O., Bonnefond, M., VanRullen, R., 2012. An oscillatory mechanism for prioritizing salient unattended stimuli. *Trends Cogn. Sci.* 16, 200–206.

Johnston, A., Nishida, S., 2001. Time perception: brain time or event time? *Curr. Biol.* 11, R427–R430.

Karmarkar, U.R., Buonomano, D.V., 2007. Timing in the absence of clocks: encoding time in neural network states. *Neuron* 53, 427–438.

Keil, A., Debener, S., Gratton, G., Junghöfer, M., Kappenman, E.S., Luck, S.J., Luu, P., Miller, G.A., Yee, C.M., 2013. Committee report: publication guidelines and recommendations for studies using electroencephalography and magnetoencephalography. *Psychophysiology* 51, 1–21.

Knudsen, E., Brainard, M., 1991. Visual instruction of the neural map of auditory space in the developing optic tectum. *Science* 253, 85–87.

- 838 Kösem, A., van Wassenhove, V., 2012. Temporal structure in audiovisual sensory selec- 909
839 tion. *PLoS One* 7, e40936. 910
- 840 Lachaux, J.P., Rodriguez, E., Martinerie, J., Varela, F.J., 1999. Measuring phase synchrony in 911
841 brain signals. *Hum. Brain Mapp.* 8, 194–208. 912
- 842 Lakatos, P., Karmos, G., Mehta, A.D., Ulbert, I., Schroeder, C.E., 2008. Entrainment of neuro- 913
843 nal oscillations as a mechanism of attentional selection. *Science* 320, 110–113. 914
- 844 Lewald, J., Guski, R., 2003. Cross-modal perceptual integration of spatially and temporally 915
845 disparate auditory and visual stimuli. *Cogn. Brain Res.* 16, 468–478. 916
- 846 Lin, F.-H., Belliveau, J.W., Dale, A.M., Hämäläinen, M.S., 2006. Distributed current estimates 917
847 using cortical orientation constraints. *Hum. Brain Mapp.* 27, 1–13. 918
- 848 Lisman, J., 2005. The theta/gamma discrete phase code occurring during the hippocampal 919
849 phase precession may be a more general brain coding scheme. *Hippocampus* 15, 920
850 913–922. 921
- 851 Lisman, J.E., Jensen, O., 2013. The theta-gamma neural code. *Neuron* 77, 1002–1016. 922
- 852 Love, S.A., Petrini, K., Cheng, A., Pollick, F.E., 2013. A psychophysical investigation of differ- 923
853 ences between synchrony and temporal order judgments. *PLoS One* 8, e54798. 924
- 854 Luo, H., Liu, Z., Poeppel, D., 2010. Auditory cortex tracks both auditory and visual stimulus 925
855 dynamics using low-frequency neuronal phase modulation. *PLoS Biol.* 8, e1000445. 926
- 856 Madl, T., Baars, B.J., Franklin, S., 2011. The timing of the cognitive cycle. *PLoS One* 6, 927
857 e14803. 928
- 858 Maris, E., Oostenveld, R., 2007. Nonparametric statistical testing of EEG- and MEG-data. 929
859 *J. Neurosci. Methods* 164, 177–190. 930
- 860 McDonald, J.J., Teder-Sälejärvi, W.A., Di Russo, F., Hillyard, S.A., 2005. Neural basis of 931
861 auditory-induced shifts in visual time-order perception. *Nat. Neurosci.* 8, 1197–1202. 932
- 862 Meredith, M., Nemitz, J., Stein, B., 1987. Determinants of multisensory integration in super- 933
863 ior colliculus neurons. I. Temporal factors. *J. Neurosci.* 7, 3215–3229. 934
- 864 Mishra, J., Martinez, A., Sejnowski, T.J., Hillyard, S.A., 2007. Early cross-modal interactions 935
865 in auditory and visual cortex underlie a sound-induced visual illusion. *J. Neurosci.* 27, 936
866 4120–4131. 937
- 867 Miyazaki, M., Yamamoto, S., Uchida, S., Kitazawa, S., 2006. Bayesian calibration of simulta- 938
868 neity in tactile temporal order judgment. *Nat. Neurosci.* 9, 875–877. 939
- 869 Monto, S., Palva, S., Voipio, J., Palva, J.M., 2008. Very slow EEG fluctuations predict the dy- 940
870 namics of stimulus detection and oscillation amplitudes in humans. *J. Neurosci.* 28, 941
871 8268–8272. 942
- 872 Morillon, B., Kell, C.A., Giraud, A.-L., 2009. Three stages and four neural systems in time es- 943
873 timation. *J. Neurosci.* 29, 14803–14811. 944
- 874 Moutoussis, K., Zeki, S., 1997. A direct demonstration of perceptual asynchrony in vision. 945
875 *Proc. Biol. Sci.* 264, 393–399. 946
- 876 Nadasdy, Z., 2010. Binding by asynchrony: the neuronal phase code. *Front. Neurosci.* 4. 947
- 877 Navarra, J., Hartcher-O'Brien, J., Piazza, E., Spence, C., 2009. Adaptation to audiovisual 948
878 asynchrony modulates the speeded detection of sound. *Proc. Natl. Acad. Sci. U. S. A.* 949
879 106, 9169–9173. 950
- 880 Neuling, T., Rach, S., Wagner, S., Wolters, C.H., Herrmann, C.S., 2012. Good vibrations: os- 951
881 cillatory phase shapes perception. *NeuroImage* 63, 771–778. 952
- 882 Nozaradan, S., Peretz, I., Missal, M., Mouraux, A., 2011. Tagging the neuronal entrainment 953
883 to beat and meter. *J. Neurosci.* 31, 10234–10240. 954
- 884 Panzeri, S., Brunel, N., Logothetis, N.K., Kayser, C., 2010. Sensory neural codes using 955
885 multiplexed temporal scales. *Trends Neurosci.* 33, 111–120. 956
- 886 Pöppel, E., 1997. A hierarchical model of temporal perception. *Trends Cogn. Sci.* 1, 56–61. 957
- 887 Rees, A., Green, G.G.R., Kay, R.H., 1986. Steady-state evoked responses to sinusoidally 958
888 amplitude-modulated sounds recorded in man. *Hear. Res.* 23, 123–133. 959
- 889 Regan, D., 1966. Some characteristics of average steady-state and transient responses 960
890 evoked by modulated light. *Electroencephalogr. Clin. Neurophysiol.* 20, 238–248. 961
- 891 Roelfsema, P., Engel, A., Konig, P., Singer, W., 1997. Visuomotor integration is associated 962
892 with zero time-lag synchronization among cortical areas. *Nature* 385, 157–161. 963
- 893 Romei, V., Gross, J., Thut, G., 2012. Sounds reset rhythms of visual cortex and correspond- 964
894 ing human visual perception. *Curr. Biol.* 22, 807–813. 965
- 895 Roopun, A.K., Kramer, M.A., Carracedo, L.M., Kaiser, M., Davies, C.H., Traub, R.D., Kopell, 966
896 N.J., Whittington, M.A., 2008. Temporal interactions between cortical rhythms. 967
897 *Front. Neurosci.* 2, 145–154. 968
- 898 Scharnowski, F., Rees, G., Walsh, V., 2013. Time and the brain: neurorelativity: the 969
899 chronoarchitecture of the brain from the neuronal rather than the observer's per- 970
900 spective. *Trends Cogn. Sci.* 17, 51–52. 971
- 901 Schroeder, C.E., Lakatos, P., 2009. Low-frequency neuronal oscillations as instruments of 972
902 sensory selection. *Trends Neurosci.* 32, 9–18. 973
- 903 Senkowski, D., Schneider, T.R., Foxe, J.J., Engel, A.K., 2008. Crossmodal binding through 974
904 neural coherence: implications for multisensory processing. *Trends Neurosci.* 31, 975
905 401–409. 976
- 906 Shaw, M.E., Hämäläinen, M.S., Gutschalk, A., 2013. How anatomical asymmetry of human 977
907 auditory cortex can lead to a rightward bias in auditory evoked fields. *NeuroImage* 978
908 74, 22–29. 979
- Skaggs, W.E., Knierim, J.J., Kudrimoti, H.S., McNaughton, B.L., 1995. A model of the neural 909
basis of the rat's sense of direction. *Adv. Neural Inf. Process. Syst.* 7, 173–180. 910
- Slutsky, D.A., Recanzone, G.H., 2001. Temporal and spatial dependency of the ventrilo- 911
quism effect. *Neuroreport* 12, 7–10. 912
- Stefanics, G., Hangya, B., Hernádi, I., Winkler, I., Lakatos, P., Ulbert, I., 2010. Phase entrain- 913
ment of human delta oscillations can mediate the effects of expectation on reaction 914
speed. *J. Neurosci.* 30, 13578–13585. 915
- Stone, J.V., Hunkin, N.M., Porrill, J., Wood, R., Keeler, V., Beanland, M., Port, M., Porter, N.R., 916
2001. When is now? Perception of simultaneity. *Proc. Biol. Sci.* 268, 31–38. 917
- Sugita, Y., Suzuki, Y., 2003. Implicit estimation of sound-arrival time. *Nature* 421. 918
- Summerfield, C., Trittschuh, E.H., Monti, J.M., Mesulam, M.M., Egner, T., 2008. Neural rep- 919
etition suppression reflects fulfilled perceptual expectations. *Nat. Neurosci.* 11, 920
1004–1006. 921
- Summerfield, C., Wyart, V., Johnen, V.M., de Gardelle, V., 2011. Human Scalp electroen- 922
cephalography reveals that repetition suppression varies with expectation. *Front.* 923
Hum. Neurosci. 5, 67. 924
- Tallon-Baudry, C., Bertrand, O., 1999. Oscillatory gamma activity in humans and its role in 925
object representation. *Trends Cogn. Sci.* 3, 151–162. 926
- Taulu, S., Kajola, M., Simola, J., 2003. Suppression of interference and artifacts by the signal 927
space separation method. *Brain Topogr.* 16, 269–275. 928
- Thorne, J.D., De Vos, M., Viola, F.C., Debener, S., 2011. Cross-modal phase reset predicts au- 929
ditory task performance in humans. *J. Neurosci.* 31, 3853–3861. 930
- Todorovic, A., de Lange, F.P., 2012. Repetition suppression and expectation suppression 931
are dissociable in time in early auditory evoked fields. *J. Neurosci.* 32, 13389–13395. 932
- Treisman, M., 1963. Temporal discrimination and the indifference interval: Implications 933
for a model of the "internal clock". *Psychol. Monogr. Gen. Appl.* 77, 1. 934
- Treisman, M., 1984. Temporal rhythms and cerebral rhythms. *Ann. N. Y. Acad. Sci.* 423, 935
542–565. 936
- Treisman, A., 1996. The binding problem. *Curr. Opin. Neurobiol.* 6, 171–178. 937
- Treisman, M., Faulkner, A., Naish, P.L., Brogan, D., 1990. The internal clock: evidence for a 938
temporal oscillator underlying time perception with some estimates of its character- 939
istic frequency. *Perception* 19, 705–743. 940
- Treisman, M., Faulkner, A., Naish, P.L.N., 1992. On the relation between time perception 941
and the timing of motor action: evidence for a temporal oscillator controlling the 942
timing of movement. *Q. J. Exp. Psychol. A* 45, 235–263. 943
- Uusitalo, M.A., Ilmoniemi, R.J., 1997. Signal-space projection method for separating MEG 944
or EEG into components. *Med. Biol. Eng. Comput.* 35, 135–140. 945
- Van Eijk, R.L.J., Kolhtrausch, A., Juola, J.F., Van de Par, S., 2008. Audiovisual synchrony and 946
temporal order judgments: effects of experimental method and stimulus type. *Percept.* 947
Psychophys. 70, 955–968. 948
- Van Wassenhove, V., 2009. Minding time in an amodal representational space. *Philos.* 949
Trans. R. Soc. Lond. B Biol. Sci. 364, 1815–1830. 950
- VanRullen, R., Koch, C., 2003. Is perception discrete or continuous? *Trends Cogn. Sci.* 7, 951
207–213. 952
- VanRullen, R., Reddy, L., Koch, C., 2006. The continuous wagon wheel illusion is associated 953
with changes in electroencephalogram power at approximately 13 Hz. *J. Neurosci.* 26, 954
502–507. 955
- Varela, F., Toro, A., John, E.R., Schwartz, E., 1981. Perceptual framing and cortical alpha 956
rhythm. *Neuropsychologia* 19, 675–686. 957
- Vibell, J., Klinge, C., Zampini, M., Spence, C., Nobre, A.C., 2007. Temporal order is coded 958
temporally in the brain: early event-related potential latency shifts underlying 959
prior entry in a cross-modal temporal order judgment task. *J. Cogn. Neurosci.* 19, 960
109–120. 961
- Vroomen, J., Keetels, M., 2010. Perception of intersensory synchrony: a tutorial review. 962
Atten. Percept. Psychophys. 72, 871–884. 963
- Vroomen, J., Keetels, M., de Gelder, B., Bertelson, P., 2004. Recalibration of temporal order 964
perception by exposure to audio-visual asynchrony. *Brain Res. Cogn. Brain Res.* 22, 965
32–35. 966
- Wang, X., 2010. Neurophysiological and computational principles of cortical rhythms in 967
cognition. *Phys. Rev. E* 81, 1195–1268. 968
- Watkins, S., Shams, L., Tanaka, S., Haynes, J.-D., Rees, G., 2006. Sound alters activity in 969
human V1 in association with illusory visual perception. *NeuroImage* 31, 1247–1256. 970
- Witten, I.B., Knudsen, E.I., 2005. Why seeing is believing: merging auditory and visual 971
worlds. *Neuron* 48, 489–496. 972
- Wittmann, M., 2009. The inner experience of time. *Philos. Trans. R. Soc. Lond. B Biol. Sci.* 973
364, 1955–1967. 974
- Wittmann, M., 2013. The inner sense of time: how the brain creates a representation of 975
duration. *Nat. Rev. Neurosci.* 14, 217–223. 976
- Yamamoto, S., Miyazaki, M., Iwano, T., Kitazawa, S., 2012. Bayesian calibration of simulta- 977
neity in audiovisual temporal order judgments. *PLoS One* 7, e40379. 978
- Zeki, S., Bartels, A., 1998. The asynchrony of consciousness. *Proc. Biol. Sci.* 265, 1583–1585. 979